

Received August 26, 2019, accepted October 14, 2019, date of publication October 30, 2019, date of current version November 12, 2019.

Digital Object Identifier 10.1109/ACCESS.2019.2950556

Ultrafast X-Ray Detector and Its Gain Uniformity

HOUZHI CAI¹, POKUN DENG, WENYONG FU, DONG WANG, AND JINYUAN LIU

Key Laboratory of Optoelectronic Devices and Systems of Ministry of Education and Guangdong Province, Shenzhen University, Shenzhen 518060, China
College of Physics and Optoelectronic Engineering, Shenzhen University, Shenzhen 518060, China

Corresponding author: Jinyuan Liu (ljy@szu.edu.cn)

This work was supported in part by the National Natural Science Foundation of China under Grant 11775147 and Grant 11705119, in part by the Science and Technology Plan Project of Shenzhen under Grant JCYJ20180305125443569 and Grant JCYJ20170818141442145, and in part by the Natural Science Foundation of Guangdong Province under Grant 2017A030310142.

ABSTRACT An ultrafast x-ray detector consisted of an electron pulse time-dilation device, a combined electromagnetic lens system, a microchannel plate (MCP) gated imager, and an electrical pulse generator is reported. The time-dilation device is used to magnify the temporal width of the electron beam created from the photo-cathode (PC), and then the combined electromagnetic lens system images the dilated electron beam onto the MCP. Finally, the MCP imager samples the dilated electron signal and outputs corresponding visible light. A measured temporal resolution of 80 ps for the detector is achieved while the electron pulse is not dilated. The resolution is improved to 12 ps while an excitation pulse with 3.1 V/ps rising edge gradient is used to drive the PC to dilate the electron pulse. Moreover, the gain uniformity of the detector is also tested, which shows the gain is decreased gradually with the excitation pulse propagating on the PC and the drop in gain is about $1.7 \times$.

INDEX TERMS Gain uniformity, pulse-dilation, temporal resolution, x-ray detector.

I. INTRODUCTION

X-ray imagers based on the gated microchannel plate (MCP) are two dimensional ultrafast detectors, and have been used in the inertial confinement fusion (ICF) or fast Z-pinch experiments successfully [1]–[8]. Such imager forms microstrip lines on the MCP to transmit the gating pulses. The incident signal is sampled and gained by the MCP while the gating pulse travels on the microstrip line to achieve the time-resolved [9]. The imagers with 35-100 ps resolution have been developed in the past decades [9], [10]. However, that temporal resolution does not meet the current ICF needs, such as the imploding ICF cores with 100 ps duration x-ray emission “hotspots” [11], [12]. The “hotspots” cannot be detected in detail by those imagers. A new faster imager is demanded to capture “hotspots” precisely. Lately, an ultrafast x-ray imager with name of DIXI has been developed [13]–[15]. It uses an electron pulse-dilation to improve the temporal resolution to be better than 10 ps. Different from the traditional imager with photo-cathode (PC) directly deposited on the MCP, the PC is divided from MCP in the DIXI, and there is an anode mesh between them. The gap between PC and mesh is an electron acceleration region, and

the area from anode mesh to MCP is an electron drift space. A negative direct-current (DC) bias voltage plus a pulse voltage are loaded on the PC, while the mesh is grounded. Therefore, an electric field varying with time is achieved between them. The potential difference between PC and mesh is decreased gradually while the photoelectron emits from PC, which produce an electron energy dispersion. The electron generated earlier obtains higher energy than the later one, and travels with a larger speed in the electron drift space. Then, the electron temporal width is magnified while they are arriving at the MCP. Finally, the MCP imager samples the dilated electron signal and outputs corresponding visible light [15]. And a higher temporal resolution is achieved.

An ultrafast x-ray detector using electron pulse-dilation is presented, and the temporal resolution as well as the gain uniformity are provided in this paper. The detector here is extended and improved from the previous one [16]. There are five different points in this detector compared to the previous camera, as shown in Table 1. Firstly, the photo-cathodes of previous camera were formed on a quartz glass window with diameter of 56 mm. The x-ray cannot pass through the silica window. Therefore, it was an ultraviolet (UV) PC, and cannot be used in the ICF experiments to measure x-rays. It can be used in the laboratories for the camera’s performance testing only. Here, the photo-cathodes are deposited onto a C_8H_8 film

The associate editor coordinating the review of this manuscript and approving it for publication was Wei Wei¹.

TABLE 1. Differences between present detector and previous camera.

Parameter	Previous camera	Present detector
PC type	ultraviolet PC	x-ray PC
PC width and valid length	8 mm, 34 mm	12 mm, 68 mm
magnetic lens number	one	two
image ratio	1:1	2:1
PC driven pulse	negative pulse with 350 ps rising edge	positive pulse with 1.4 ns rising edge

with diameter of 90 mm to form an x-ray PC. Moreover, each UV PC with 8 mm width was used in the previous camera, and the valid PC length was about 34 mm. In this detector, the width of each x-ray PC is 12 mm, and the valid PC length is lengthened to 68 mm. The PC sensitive area here is larger than that of the previous UV PC. The current detector can capture the ICF “hotspots” with a longer record in time to obtain a more detailed and precise ICF results [17]. Certainly, the larger PC sensitive area can bring a larger size for the ICF implosion image, and a higher spatial resolution could be achieved [17]. Furthermore, only one magnetic lens was used in the previous camera. In this paper, there are two large aperture magnetic lenses to form a combined electromagnetic lens system, which can bring a higher spatial resolution and a larger imaging area with high quality. In addition, the image ratio for the electrons from PC onto MCP was 1:1 in the previous camera. In the present detector, an image ratio of 2:1 is formed, which can achieve a larger PC size while using the same MCP. Finally, the PC was driven by a negative pulse with 350 ps rising edge in the previous camera to obtain the electron time-dilation. In the current detector, a positive pulse with 1.4 ns rising edge is used. In the ICF experiment with about 1-2 ns duration, the rising edge with 1.4 ns is better than that of 350 ps.

II. DETECTOR ARCHITECTURE

The ultrafast x-ray detector is composed of four parts, an electron pulse time-dilation device, an electrical pulse generator, a MCP gated imager, and a combined electromagnetic lens system, shown in Fig. 1. The electron pulse time-dilation device is consisted of three strip-line photo-cathodes, a grounded anode mesh, and an electron drift region. The microstrip transmission line x-ray photo-cathodes are formed by 80 nm gold deposited on the C_8H_8 film with 90 mm diameter. Each PC has 12 mm width, and a 10 mm gap for the two adjacent cathodes is used. The PC excitation pulse outputted from the electrical pulse generator is transmitted to the input port connector of the time-dilation device, and then to a microstrip transmission line with tapered structure manufactured on the printed circuit board. The tapered transmission line is connected with PC by a gold foil. Finally, the PC excitation pulse is transmitted to the PC to achieve an electron time-dilation. In the output side, the tapered transmission line guides the PC excitation pulse to the output terminal.

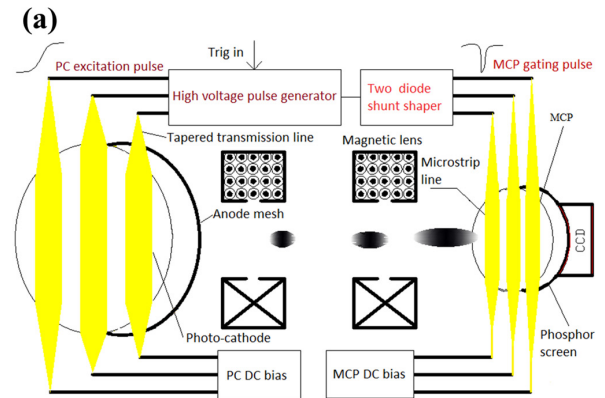
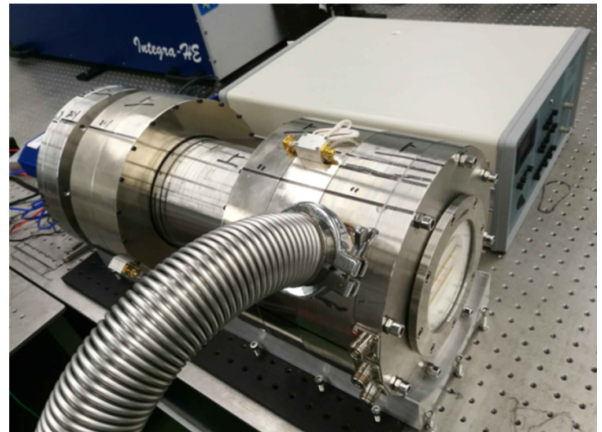
**(b)**

FIGURE 1. (a) Structural diagram of the ultrafast x-ray detector. (b) Photograph of the ultrafast x-ray detector.

The accelerating gap from PC to mesh is 1.5 mm. An excitation pulse overlapped with a negative DC high voltage are applied on the PC, while the anode mesh is ground potential, which creates an electron energy dispersion. The mesh is electroformed nickel with a spatial frequency of 10 lp/mm. An electron drift space with length of 50 cm is used between mesh and MCP. The electrons generated earlier travel faster in the drift space, which produces a dilated electron beam.

The combined electromagnetic lens system is formed by two identical electromagnetic lenses with a large aperture. This system images photoelectrons from PC onto MCP, and an image de-magnification of two times is achieved. Such imaging system can obtain a better imaging quality and focusing ability of optical electronic, and it has been successfully used in the streak cameras and electron microscopes [18]–[20]. The front electromagnetic lens with an excitation current of 0.198 A is mounted at the place 7.5 cm from the PC. The gap between the back lens and the MCP is 4 cm, and the excitation current applied on the back lens is 0.31 A. Each electromagnetic lens has 1320-turn copper coil windings. The outside surface of the windings is enclosed by a soft iron shield with a 4 mm lens gap in the inner round surface. The outer diameter, inner diameter, and axial length of the lens are respectively 256 mm, 160 mm, and 100 mm.

The magnetic field passes through the 4 mm lens gap to the electron drift space. Then, a magnetic lens is formed, which leads to achieve a non-uniform axisymmetric magnetic field. The on-axis magnetic field strength distribution generated by every lens is an approximate normal distribution [16].

The MCP gated imager is made up of a gated MCP, a phosphor screen, and a charge-coupled device (CCD). The MCP with 56 mm diameter and 0.5 mm thickness is used. The diameter of the MCP pore is 12 μm , and the bias angle of the MCP is 6° . The microstrip transmission lines are coated with 5000 \AA copper overlaid by 1000 \AA gold on the MCP surface. The gating pulse moves along the transmission line to sample the incident signal, and then a MCP gate width is achieved [21]. Each MCP transmission line has a width of 8 mm, and a gap of 3 mm between two adjacent transmission lines is formed. Similar to the time-dilation device, the gating pulse is transmitted from the input port to the MCP transmission line by a tapered microstrip transmission line. The other MCP surface is also deposited with copper and gold, and the whole surface is ground potential. The gained electrons are outputted from this grounded MCP surface to hit the phosphor screen. The phosphor screen with 4 kV positive DC voltage is mounted 0.5 mm to the MCP output surface. The CCD is contacted with phosphor screen, and captures the visible image.

The electrical pulse generator outputs a gating pulse to MCP and an excitation pulse to PC. Firstly, some avalanche transistors are constructed as Marx bank circuit to create high voltage pulses with short rise time. One high voltage pulse is outputted to the pulse time-dilation device and used to drive PC. The other high voltage pulse is transmitted to an avalanche diodes shaped circuit to produce MCP gating pulse [22]. The PC excitation pulse with a gradient of 3.1 V/ps is achieved, shown in Fig. 2(a). The MCP gating pulse shape is shown in Fig. 2(b), has an amplitude of -1.8 kV and a width of 225 ps.

III. TEMPORAL RESOLUTION MEASUREMENT

The temporal resolution is considered as the width of the gain curve. The measured setup for the temporal resolution was described in the previous paper [16]. The actual application of this detector in ICF experiment is detecting x-rays. However, we lack x-ray source for the temporal resolution and gain uniformity measurement. Therefore, the performance is characterized utilizing a UV laser, which has been used in the previous camera test [10], [13], [16]. The temporal resolution or gain uniformity is almost the same as that acquired by x-ray test. The incident x-ray or UV laser is converted to photoelectrons. The x-ray will produce a larger electron energy distribution. However, the initial electron energy distribution is much less than the energy dispersion achieved by the time-dilation device. Therefore, the performance difference caused by the x-ray or UV laser test could be negligible. The performance is mainly determined by four factors, the PC bias voltage, the PC excitation pulse gradient, the drift length, and the MCP gate width [13]–[16]. The laser system can

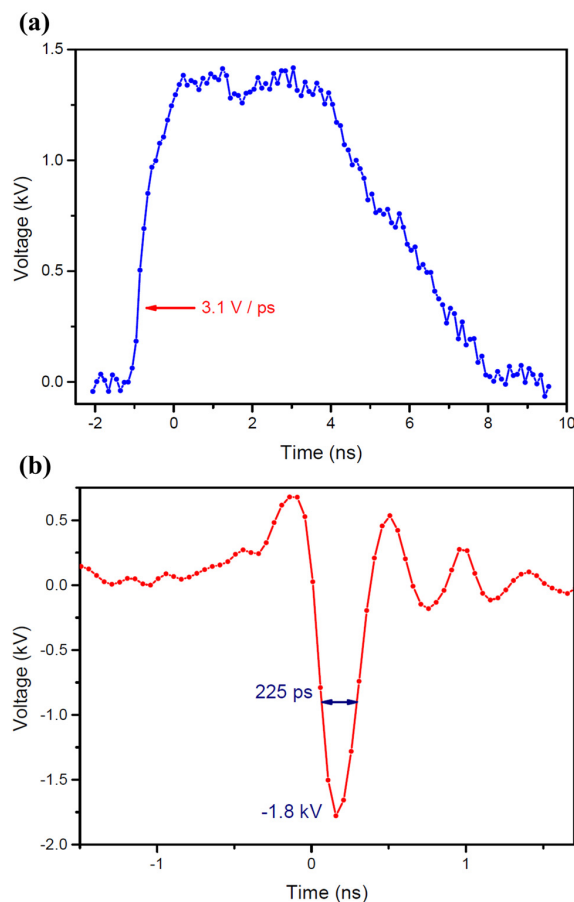


FIGURE 2. (a) The shape of the excitation pulse applied on PC with a gradient of 3.1 V/ps. (b) The MCP gating pulse shape with an amplitude of -1.8 kV and a width of 225 ps.

output 800 and UV 266 nm laser beams. The 266 nm laser pulse with width of 130 fs is firstly delayed by the air optical path and then reflected by a 45 degree UV total reflection mirror M_2 . The reflected light travels to the fiber bundle with thirty different length fibers to output thirty laser pulses at different time. Here, the time-delay of 10 ps between each two neighboring fibers is used. Finally, the thirty laser pulses are imaged from fiber bundle to PC by the convex lenses L_1 and L_2 to generate thirty photoelectron pulses with different birth time. The 800 nm laser pulse is reflected by an infrared 45 degree total reflection mirror M_1 , and the reflected light propagates to a PIN to create an electrical pulse. This electrical pulse triggers the electrical pulse generator to output PC excitation and MCP gating pulses. The delay circuit adjusts the electrical pulse trigger time to synchronize the thirty laser pulses with the PC excitation pulse rising edge. Then, the dilated electron pulses are synchronized with the MCP gating pulse to achieve a gating image.

While a -3 kV DC voltage is for the PC, and -700 V DC voltage is applied on MCP. The fiber bunch static image is shown in Fig. 3(a). While there is a -3 kV DC voltage for the PC, and a -400 V DC bias voltage overlapped with the gating pulse for the MCP, the fiber bunch gating

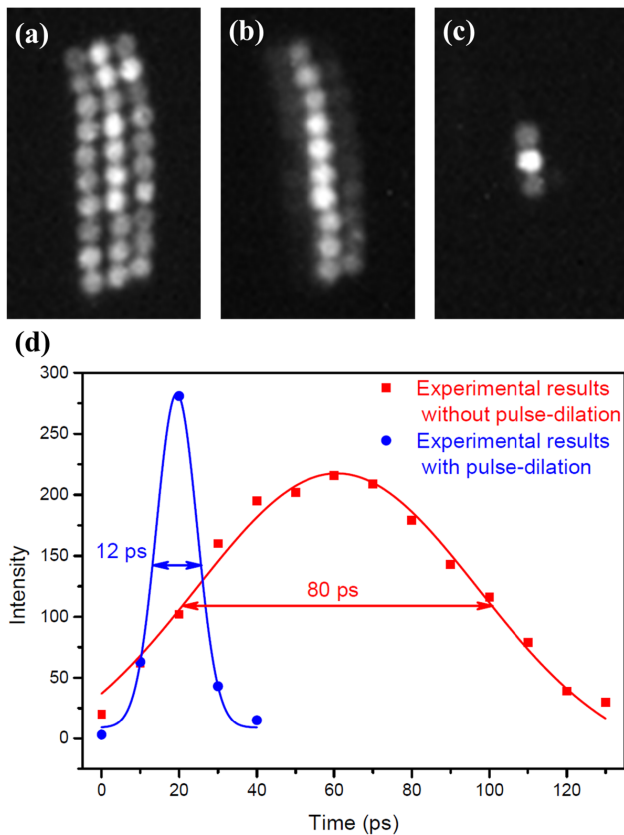


FIGURE 3. (a) Static image of the fiber bunch, the PC is applied with -3 kV DC voltage, and a -700 V DC voltage is on MCP. (b) Gating image while the PC is without excitation pulse, the PC is applied with -3 kV DC voltage, and the MCP is with a -400 V DC bias voltage plus the gating pulse. (c) Gating image while the electron beam is dilated, the PC is with excitation pulse plus a -3 kV DC bias voltage, the MCP is applied with the same voltages as that for (b). (d) Signals out of the fiber bunch gating image while no electron beam dilated in (b) and gating image while the electron beam is dilated in (c).

image without electron beam dilated is shown in Fig. 3(b). Furthermore, while the PC is with a -3 kV DC bias plus the excitation pulse, and the MCP is applied with the same voltages as that for Fig. 3(b), the fiber bunch gating image with electron pulse-dilation is shown in Fig. 3(c). The images in Figs. 3(a)–3(c) are original picture outputted from CCD. The gating results in Figs. 3(b) and 3(c) are calibrated by the static image in Fig. 3(a), and the calibrated gating image intensity is plotted as shown in Fig. 3(d). The square points in Fig. 3(d) are the experimental results from Fig. 3(b), and the circle points are from Fig. 3(c). The lines are the Gaussian fits for the points. It can be seen from Fig. 3(d) that while the electron pulse is not dilated, a temporal resolution of 80 ps is achieved for the MCP imager. And the temporal resolution of the ultrafast x-ray detector is improved to 12 ps with electron pulse-dilation technology.

IV. GAIN UNIFORMITY MEASUREMENT

In the ultrafast x-ray detector, there are two factors which could influence the gain uniformity. One is that the excitation pulse is experienced with gradually decreased amplitude

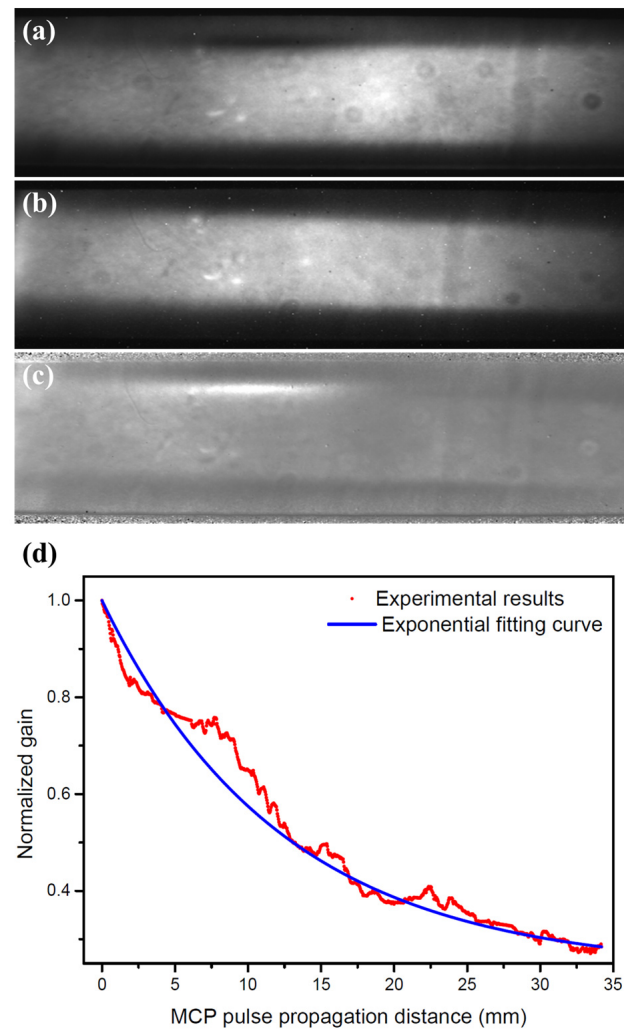


FIGURE 4. (a) Static image of the microstrip line cathode, only a -3 kV DC voltage is on the PC, and the MCP is with a DC voltage of -700 V. This is an integral image with 5 shots. (b) Gating image of the microstrip line cathode without pulse-dilation, a -3 kV DC voltage is on PC, and the gating pulse plus a -400 V DC voltage is on MCP. It is a 40 shots integral image. The MCP gating pulse propagates from left to right. (c) The final microstrip line cathode gating image without pulse-dilation, while (a) is used to calibrate (b). (d) Horizontal line out of the image in (c).

while it transmits on the PC, which will affect the gain uniformity. The other one is the MCP gain uniformity caused by the gradually reduced gating pulse. The experimental setup of the gain uniformity resembles the temporal resolution tested setup, but has two differences. In the gain uniformity experimental setup, the fiber bunch is not used, and the laser width is different. The UV laser pulse used in the gain uniformity measurement has 10 mJ energy and 6.5 ns width. There is a 3.2 ns flat-top. A concave lens is used to spatially expand the UV light, and then the expanded UV pulse irradiates the PC to excite photoelectrons. The PC excitation pulse is synchronized with the UV light at the flat-top center. A delay time of about 17.3 ns is used between the MCP gating and PC excitation pulses, it is the same as that in the temporal resolution measurement. While the PC is only with a DC voltage of -3 kV, and the MCP is with a DC

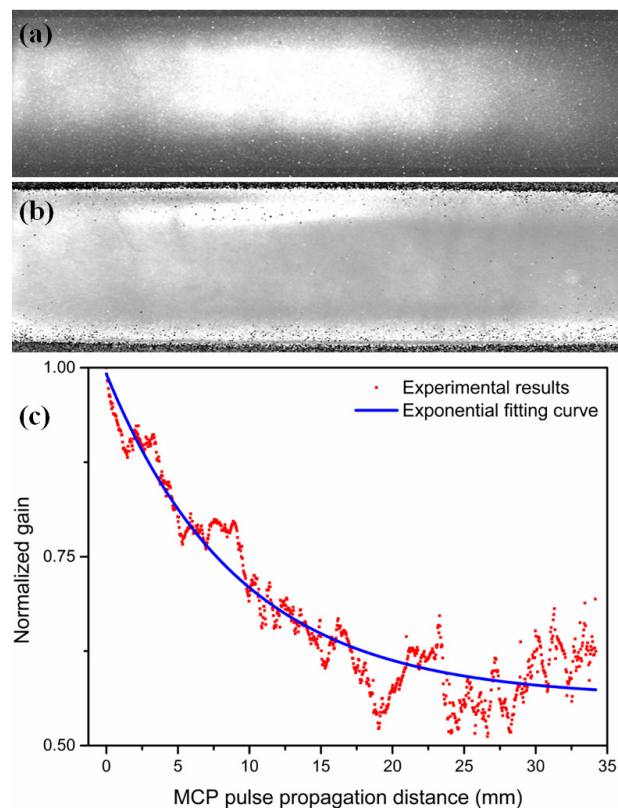


FIGURE 5. (a) Microstrip line cathode gating image with electron pulse-dilation, the PC is with an excitation pulse plus a -3 kV DC voltage, and the MCP is with the same voltages as that for Fig. 4(b). It is a 40 shots integral image. (b) The final microstrip line cathode gating image with pulse-dilation, while Fig. 4(a) is used to calibrate Fig. 5(a). (c) The results for horizontal line out of the image in (b).

voltage of -700 V, the microstrip line static image is shown in Fig. 4(a). While there is only a -3 kV DC voltage on the PC, and the MCP is with a -400 V DC voltage plus the gating pulse, the microstrip line gating image without electron beam dilated is shown in Fig. 4(b). The images in Figs. 4(a) and 4(b) are original pictures. While Fig. 4(b) is calibrated by Fig. 4(a), the final calibrated microstrip line gating image without pulse-dilation is shown in Fig. 4(c). The results for horizontal line out of Fig. 4(c) are shown in Fig. 4(d). The red circle points are measured results, and the blue line is an exponential fitting curve. Fig. 4(d) shows that the drop in gain is $3.5\times$ on the MCP transmission line. It is the gain uniformity of the MCP gated imager. The MCP gain is greatly influenced by the voltage applied on MCP. The gating pulse has voltage loss as it transmits along MCP transmission line, which leads to the dropped MCP gain [23].

While PC is with a -3 kV DC bias voltage plus the excitation pulse, and MCP is applied the same voltages as that for Fig. 4(b), the microstrip line gating image with electron pulse-dilation is obtained, as shown in Fig. 5(a). The final microstrip line gating image with electron pulse-dilation is shown in Fig. 5(b). It is obtained by calibrating the gating image in Fig. 5(a) using the static image in Fig. 4(a). Finally,

the results for horizontal line out of the image in Fig. 5(b) are acquired, as shown in Fig. 5(c). It shows that the gain is dropped $1.7\times$ along the MCP gating pulse traveling direction. It is the gain uniformity of the ultrafast x-ray detector, and is better than that of the MCP gated imager, which is due to the increasing numbers of electrons along the MCP transmission line caused by the gradually decreasing temporal magnification. The amplitude of the excitation pulse is reduced while the pulse travels on PC, which leads to a decreasing excitation pulse gradient. The decreasing pulse gradient produces a gradually decreasing temporal magnification factor along the PC transmission line [16], which leads to a gradually increasing electron density. At the electron drift space end, a MCP with the gate width of 80 ps is used to sample the dilated electron pulse. In the 80 ps gate time, the number of electrons passing through the MCP will be increased while the electron density is increased. Then, the output signal intensity along the MCP microstrip line will be raised gradually owing to the increased electron number. Therefore, the gain uniformity of the detector with electron pulse-dilation is better than the gated MCP gain uniformity.

V. CONCLUSION

An ultrafast x-ray detector with electron pulse-dilation is described. This detector has a higher temporal resolution than the conventional MCP gated imager. The gating image is acquired in single shot by using a fiber bunch with thirty different length fibers, which can avoid temporal resolution measurement error caused by timing jitter between different shots. While the PC is only with a -3 kV DC voltage, and a -400 V DC bias plus the gating pulse is on MCP, the temporal resolution without electron beam dilated is about 80 ps. While an excitation pulse is used to drive PC, a higher temporal resolution is achieved. The resolution with electron pulse-dilation is 12 ps. The gain uniformity is also one of the most important parameters. It could be used to get better quantitative precision for the x-ray image in the ICF experiment [24], [25]. The gain uniformity of the detector is tested, and the results show that the gain is dropped $1.7\times$ along the pulse transmitting direction.

REFERENCES

- [1] O. A. Hurricane et al., "Fuel gain exceeding unity in an inertially confined fusion implosion," *Nature*, vol. 506, pp. 343–348, Feb. 2014.
- [2] C. J. Cerjan et al., "Dynamic high energy density plasma environments at the national ignition facility for nuclear science research," *J. Phys. G, Nucl. Part. Phys.*, vol. 45, no. 3, Feb. 2018, Art. no. 033003.
- [3] A. Pak et al., "Examining the radiation drive asymmetries present in the high foot series of implosion experiments at the National Ignition Facility," *Phys. Plasmas*, vol. 24, no. 5, May 2017, Art. no. 056306.
- [4] D. A. Martinez et al., "Hydro-instability growth of perturbation seeds from alternate capsule-support strategies in indirect-drive implosions on National Ignition Facility," *Phys. Plasmas*, vol. 24, no. 10, Oct. 2017, Art. no. 102707.
- [5] S. R. Nagel, H. Chen, J. Park, M. Foord, A. U. Hazi, T. J. Hillsabeck, S. M. Kerr, E. V. Marley, and G. J. Williams, "Two-dimensional time-resolved ultra-high speed imaging of K-alpha emission from short-pulse-laser interactions to observe electron recirculation," *Appl. Phys. Lett.*, vol. 110, no. 14, Apr. 2017, Art. no. 144102.

- [6] V. V. Nagarkar, S. V. Tipnis, T. K. Gupta, S. R. Miller, V. B. Gaysinskiy, Y. Klugerman, M. R. Squillante, G. Entine, and W. W. Moses, "High speed X-ray imaging camera using a structured CsI(Tl) scintillator," *IEEE Trans. Nucl. Sci.*, vol. 46, no. 3, pp. 232–236, Jun. 1999.
- [7] W. Yang, X. Hou, Y. Bai, X. Bai, B. Liu, J. Zhao, and J. Qin, "A prototype X-ray framing camera with variable exposure time based on double-gated micro-channel plates," *IEEE Trans. Nucl. Sci.*, vol. 56, no. 4, pp. 2487–2492, Aug. 2009.
- [8] T. Beck, C. Zuber, D. Aubert, C. Chollet, P. Brunel, S. Huelvan, C. Brisset, and H.-P. Jacquet, "Recent advances in the development of X-ray cameras inserted inside a pressurized box for LMJ plasma diagnostics," *IEEE Trans. Plasma Sci.*, vol. 38, no. 10, pp. 2867–2872, Oct. 2010.
- [9] J. D. Kilkenny, "High speed proximity focused X-ray cameras," *Laser Part. Beams*, vol. 9, no. 1, pp. 49–69, 1991.
- [10] P. M. Bell, J. D. Kilkenny, R. L. Hanks, and O. L. Landen, "Measurements with a 35-psec gate time microchannel plate camera," *Proc. SPIE*, vol. 1346, pp. 456–464, Jan. 1990.
- [11] T. J. Hilsabeck, "Picosecond imaging of inertial confinement fusion plasmas using electron pulse-dilation," *Proc. SPIE*, vol. 10328, Feb. 2017, Art. no. 103280S.
- [12] S. R. Nagel, L. R. Benedetti, D. K. Bradley, T. J. Hilsabeck, N. Izumi, S. Khan, G. A. Kyrala, T. Ma, and A. Pak, "Comparison of implosion core metrics: A 10 ps dilation X-ray imager vs a 100 ps gated microchannel plate," *Rev. Sci. Instrum.*, vol. 87, no. 11, Nov. 2016, Art. no. 11E311.
- [13] T. J. Hilsabeck, J. D. Hares, J. D. Kilkenny, P. M. Bell, A. K. L. Dymoke-Bradshaw, J. A. Koch, P. M. Celliers, D. K. Bradley, T. McCarville, M. Pivovarov, R. Soufli, and R. Bionta, "Pulse-dilation enhanced gated optical imager with 5 ps resolution (invited)," *Rev. Sci. Instrum.*, vol. 81, no. 10, Oct. 2010, Art. no. 10E317.
- [14] S. R. Nagel, T. J. Hilsabeck, P. M. Bell, D. K. Bradley, M. J. Ayers, K. Piston, B. Felker, J. D. Kilkenny, T. Chung, B. Sammulu, J. D. Hares, and A. K. L. Dymoke-Bradshaw, "Investigating high speed phenomena in laser plasma interactions using dilation X-ray imager (invited)," *Rev. Sci. Instrum.*, vol. 85, no. 11, Nov. 2014, Art. no. 11E504.
- [15] S. R. Nagel, T. J. Hilsabeck, P. M. Bell, D. K. Bradley, M. J. Ayers, M. A. Barrios, B. Felker, R. F. Smith, G. W. Collins, O. S. Jones, J. D. Kilkenny, T. Chung, K. Piston, K. S. Raman, B. Sammulu, J. D. Hares, and A. K. L. Dymoke-Bradshaw, "Dilation X-ray imager a new/faster gated X-ray imager for the NIF," *Rev. Sci. Instrum.*, vol. 83, no. 10, Oct. 2012, Art. no. 10E116.
- [16] H. Cai, X. Zhao, J. Liu, W. Xie, Y. Bai, Y. Lei, Y. Liao, and H. Niu, "Dilation framing camera with 4 ps resolution," *APL Photon.*, vol. 1, no. 1, Apr. 2016, Art. no. 016101.
- [17] J. A. Oertel, T. Archuleta, M. S. Bakeman, P. Sanchez, G. Sandoval, L. Schrank, P. J. Walsh, and N. Pederson, "A large-format gated X-ray framing camera," *Proc. SPIE*, vol. 5194, pp. 214–222, Jan. 2004.
- [18] J. Feng, K. Engelhorn, B. I. Cho, H. J. Lee, M. Greaves, C. P. Weber, R. W. Falcone, H. A. Padmore, and P. A. Heimann, "A grazing incidence X-ray streak camera for ultrafast, single-shot measurements," *Appl. Phys. Lett.*, vol. 96, no. 13, Mar. 2010, Art. no. 134102.
- [19] I. Konvalina and I. Müllerová, "Properties of the cathode lens combined with a focusing magnetic/immersion-magnetic lens," *Nucl. Instrum. Methods Phys. Res. Sect. A, Accel., Spectrometers, Detectors Associated Equip.*, vol. 645, no. 1, pp. 55–59, Jul. 2011.
- [20] Z. Chang, A. Rundquist, J. Zhou, M. M. Murnane, H. C. Kapteyn, X. Liu, B. Shan, J. Liu, L. Niu, M. Gong, and X. Zhang, "Demonstration of a sub-picosecond X-ray streak camera," *Appl. Phys. Lett.*, vol. 69, no. 1, p. 133, Jul. 1996.
- [21] M. Koga and H. Shiraga, "Gain depletion of X-ray framing camera," *Rev. Sci. Instrum.*, vol. 88, no. 8, Aug. 2017, Art. no. 083514.
- [22] P. M. Bell, J. D. Kilkenny, O. L. Landen, R. L. Hanks, and D. K. Bradley, "Electrical characteristics of short pulse gated microchannel plate detectors," *Rev. Sci. Instrum.*, vol. 63, no. 10, p. 5072, Oct. 1992.
- [23] T. McCarville, S. Fulkerson, R. Booth, J. Emig, B. Young, S. Anderson, and B. Heeter, "Gated X-ray intensifier for large format simultaneous imaging," *Rev. Sci. Instrum.*, vol. 76, no. 10, Oct. 2005, Art. no. 103501.
- [24] L. R. Benedetti, J. P. Holder, M. Perkins, C. G. Brown, C. S. Anderson, F. V. Allen, R. B. Petre, D. Hargrove, S. M. Glenn, N. Simanovskaia, D. K. Bradley, and P. Bell, "Advances in X-ray framing cameras at the National Ignition Facility to improve quantitative precision in X-ray imaging," *Rev. Sci. Instrum.*, vol. 87, no. 2, Feb. 2016, Art. no. 023511.
- [25] J. A. Oertel and T. N. Archuleta, "A novel solution to the gated X-ray detector gain droop problem," *Rev. Sci. Instrum.*, vol. 85, no. 11, Nov. 2014, Art. no. 11D622.



HOZHUI CAI received the B.S. degree in optical information science and technology from the Huazhong University of Science and Technology, China, in 2004, and the M.S. and Ph.D. degrees in optical engineering from Shenzhen University, China, in 2007 and 2010, respectively. He is currently an Associate Professor with the College of Physics and Optoelectronic Engineering, Shenzhen University, China. His research interest includes the design and characterization of ultrafast sensors with sub-nanosecond temporal resolution.



POKUN DENG is currently pursuing the master's degree with the College of Physics and Optoelectronic Engineering, Shenzhen University, China. His research interest includes the pulse generator of ultrafast sensor.



WENYONG FU is currently pursuing the Ph.D. degree with the College of Physics and Optoelectronic Engineering, Shenzhen University, China. His research interest includes the electric circuit of ultrafast sensor.



DONG WANG currently holds a postdoctoral position with the College of Physics and Optoelectronic Engineering, Shenzhen University, China. His research interest includes the theoretical research of ultrafast sensor.



JINYUAN LIU is currently a Professor with the College of Physics and Optoelectronic Engineering, Shenzhen University, China. His research interest includes the development of devices for ultrafast sensing applications.

...